Appendix A3 – Derivation of the p + D → ^{3}He Reaction Rate

Written: 2 October 2005, minor updates 13/11/09

1. Introduction

We have noted in Chapters 13 and 14 that the crucial slowness of the reaction which initiates stellar burning of hydrogen, i.e. $p + p \rightarrow D + e^+ + \nu_e$, is due in part to the need for the protons to penetrate the Coulomb barrier before they can react. This being the case, we have queried (Chapter 14) why the second reaction, i.e. p + D → ^{3}He + γ, should not also be slow, since a Coulomb barrier needs to be penetrated in this case also. Yet these two reactions differ in rate by about a factor of 10^{17}. In this Appendix we derive the rate of the p + D → ^{3}He + γ reaction from first principles. We shall see that it is indeed suppressed by the Coulomb barrier. This is the reason for this reaction rate reducing extremely steeply, effectively switching off, below temperatures of ~10^7K. We conclude that the 17 orders of magnitude difference in the two reaction rates must actually be due entirely to the weakness of the weak nuclear force, contrary to the impression given by many popular physics books.

2. The Contributing Matrix Elements

We are dealing with a system of two protons and one neutron. The ground state of helium-3 will be an S-state. The two protons must therefore have anti-aligned spins, by the exclusion principle, so the overall spin of ^{3}He must be ½, arising from the neutron spin. In the free state, the two proton spins may alternatively be aligned, in which case, to be consistent with the exclusion principle, they must be in an odd L state.

Following the derivation of the proton-neutron matrix elements (Appendix A2) we consider two interaction Hamiltonians: the electric dipole interaction, $H_I = 2eE_0 r\cos\theta$; and the magnetic dipole interaction, $H_I = \overline{B}_0 \cdot \hat{\overline{M}}ag$, where $\hat{M}ag$ is the magnetic moment operator and E_0 and B_0 are the electric and magnetic fields due to the gamma ray photon. [In the case of photodisintegration, this is the incident radiation. In the case of proton capture, this is the emitted photon].

We firstly consider the magnetic dipole interaction. Recall from Appendix 2 that the magnetic dipole matrix element was non-zero for the n-p system only when the free state was chosen to be a spin singlet state, in contrast to the bound state (deuteron) which is a spin triplet. The spin dependence of the strong nuclear potential then leads to a non-zero matrix element. For the ppn system, considering just S-wave (L = 0) states, there is just one possible total spin state, spin ½, in which the two protons form a singlet sub-state. The matrix element between two such states of differing energy is zero, by orthogonality. Unlike the n-p system we do not have the choice between two different spin states – with differing nuclear potentials. On the other hand, if we consider the free state to be a P-wave (L = 1), and the spin state to be $^3/_2$[1], then the two states will be eigenfunctions corresponding to different (spin dependent) nuclear potentials. However, the matrix element is again zero due to the angular integral (i.e. S and P states are always orthogonal, irrespective of the radial dependence). We conclude that the magnetic dipole matrix element is identically zero (at least in first

[1] NB: The matrix element of the operator $\hat{M}ag$ between spine ½ and spin 3/2 states can be non-zero as long as the two states have the same azimuthal spin component.

order perturbation theory), essentially as a consequence of the exclusion principle. Since the magnetic term is dominant in the n-p system (accounting for 99+% of the reactions below ~10^8K, see Appendix 2) we can therefore expect the p + D $\rightarrow$ ^{3}He + γ reaction rate to be much slower than the capture of protons by neutrons (even before accounting for the Coulomb barrier).

The electric dipole matrix element is non-zero, however. In view of the presence of the cosθ factor in the interaction Hamiltonian, the only non-zero matrix element will be that in which the free state is a P-wave. The two proton spins must then be aligned, by the exclusion principle. According to whether the neutron spin is aligned or anti-aligned with the proton spins, the total spin will be $^3/_2$ or ½. However, because the bound state (^{3}He) is spin ½, and because the electric dipole interaction does not affect the spin, the spin $^3/_2$ free state will give a zero matrix element. Consequently, the only non-zero matrix element contributing in first order perturbation theory is,

$$\text{matrix element} = \; < \text{spin}^{1}/_{2}, \text{S(bound)} \left| eE_0 r \cos\theta \right| \text{spin}^{1}/_{2}, \text{P(free)} > \qquad \text{(Equ.1)}$$

noting that the factor of 'r' in the interaction Hamiltonian is what prevents orthogonality making the radial integration zero. Note that Equ.1 is the matrix element factor per proton, i.e. a charge of just 'e' has been assumed. Since there are two protons, this matrix element is duplicated for the other proton.

The fact that the spin state is the same for the free state as for the bound state is fortunate. This is because we do not yet know what the effective nuclear potential is for ^{3}He. We can, however, determine the effective potential for the spin ½ state (or, rather, we can determine possible pairs of V_0 and a) from the measured binding energy of ^{3}He. This same potential & range combination will apply also for the free state because it is also spin ½. Had the spin $^3/_2$ free state been involved, we would have had a difficulty determining the effective potential and range for this spin state.

3. Effective Nuclear Potential For ^{3}He

The radial Schrodinger equation is,

$$\left[\frac{\hbar^2}{2m} \partial_r^2 - \frac{\hbar^2}{2m} \cdot \frac{L(L+1)}{r^2} - V(r) + E \right] u(r) = 0 \qquad \text{where, } \psi = \frac{u}{r} \qquad \text{(Equ.2)}$$

Now, to write a Schrodinger equation in just one (radial) coordinate, we must be assuming a two-body problem. Strictly, we are now dealing with a three-body problem, two protons and a neutron. However, we intend to treat the deuteron as if it were a single particle in its own right. The two-body system in question is therefore the p-D system. Since these two particles are of mass M_p and $2M_p$ (approximately), the reduced mass m is just ($^2/3$)M_p.

A positive potential is repulsive, so the centrifugal force is seen to be repulsive, as it should be. In the simple square-well model for the nuclear force we have,

$$V(r) = -V_0 \qquad \text{for} \qquad r < a \qquad \text{(Equ.3a)}$$

$$V(r) = \frac{Z(Z-1)}{2} \cdot \frac{\tilde{e}^2}{r} \quad \text{for } r > a \qquad \text{(Equ.3b)}$$

For the deuteron, Z = 1 and the Coulomb potential does not contribute. For helium, Z = 2 and the Coulomb potential is $\tilde{e}^2 / r$. We have $\tilde{e}^2 = 1.44$ MeVfm.

The known binding energy of helium-3 is B = 7.7180MeV. We have numerically integrated the Schrodinger equation (EXCEL macro NSW1a) to find combinations of V_0 and a which reproduce this binding energy to at least 4 decimal places. These are given in the Table below. The Table also shows the values of $-a\alpha\cot(a\alpha)$ and $a\beta$, where $(\hbar\beta)^2 = 2mB$ and $(\hbar\alpha)^2 = 2m(V_0 - B)$. These two quantities would be equal if it were not for the influence of the Coulomb potential. It can be seen that they are quite close, which shows that the Coulomb potential does not have a dramatic effect on the binding energy, though it does have a noticeable effect. The numerical integration applied the boundary condition near the origin at r = 0.001 fm and used an integration step size (Δr) of 0.01 fm. Sensitivity to a change to a step size (Δr) of 0.0025 fm caused a change in the required V_0 to reproduce the required binding energy of only 0.08%.

Effective Nuclear Potential And Range For ^{3}He

a (fm)	**V_0 (MeV)**	$-a\alpha\cot(a\alpha)$	**$a\beta$**
4	17.99	2.0287	1.9891
3	24.231		
2	40.14	1.0294	0.9946
1.5	60.498		
1.2	85.247	0.6278	0.5968
1.0	114.364		
0.8	166.216	0.4259	0.3978

Note that there is no simple combination of V_0 and a (e.g. a^2V_0) which is invariant. There was no other bound state of helium-3 for the above potentials (i.e. no excited states of helium-3, which I believe is in fact the case).

If the above prescription for the nuclear 3-body problem were correct, we would expect to be able to derive the binding energy of tritium (pnn) from the same potential & range combinations just by switching off the Coulomb potential. The actual binding energy of tritium is 8.4818 MeV, some 0.7638 MeV larger than that of helium-3. The sign of this binding energy difference is as we would expect, being due to the repulsive nature of the Coulomb force causing helium-3 to be less tightly bound. Running NSW1a with the Coulomb potential switched off, and for nuclear force ranges of 4, 2, 1 and 0.6 fm, gives increases in binding energy of 0.056, 0.207, 0.527 and 0.676 MeV respectively. We see that, for the shortest ranges we are indeed approaching the correct binding energy difference (0.7638 MeV). The lesson from this observation is that for nuclei larger than the deuteron, the absolute size (a) is significant in determining nuclear properties.

4. Numerical Evaluation Of Matrix Elements

In the case of the n-p system we used the zero-range approximation to find algebraic expressions for the matrix elements (see Appendix 2). This was possible because we have simple, exact, analytic solutions for the wavefunctions in the absence of a Coulomb potential. Unfortunately, the presence of the Coulomb potential makes it preferable to resort to numerical solutions. The EXCEL macro NSW1b has been used. Before proceeding to the p + D reaction, we carry out checks on the numerical procedure by reproducing the analytical results for the n-p system.

4.1 Check of Program NSW1b Against n-p Matrix Elements

For application to the p-D system we shall only need the electric dipole matrix element between the bound S state and a free P state, both of the same spin state (hence the same nuclear potential). However, for completeness, the program NSW1b is also checked here for the case of the magnetic dipole matrix element between two S states of different spin (i.e. different nuclear potentials). We start with the latter.

4.1.1 Check of $<^3 \mathrm{S(bound)}\left|{}^1\mathrm{S(free)}\right.>$ For The n-p Potentials

Recall first of all that matrix elements involving free states are defined only if a normalisation volume is specified. The matrix element has been determined in Appendix A2 to be,

$$<^3 \mathrm{S(bound)}\left|{}^1\mathrm{S(free)}\right.>\Big|_{\mathrm{n-p}} = 2\left(\frac{\beta-\tilde{\beta}}{k^2+\beta^2}\right)\sqrt{\frac{\beta}{\left(1+\tilde{B}/E\right)r_{max}}} \qquad \text{(Equ.3)}$$

where, $(\hbar\beta)^2 = 2mB$, B is the deuteron binding energy (2.2245MeV), $(\hbar\tilde{\beta})^2 = 2m\tilde{B}$, and also $\tilde{\beta} = 1/{}^1a$, where ${}^1a$ is the n-p singlet scattering length, i.e. –23.69fm. Hence, $\tilde{\beta} = -0.04221\mathrm{fm}^{-1}$, and $\tilde{B} = +0.07415\mathrm{MeV}$. E is the total energy of the two nucleons in the cms system (the eigenvalue of the Schrodinger equation), and $(\hbar k)^2 = 2mE$. Finally, r_{max} is the radius of the normalisation volume. The numerical value of the matrix element is meaningless without r_{max} being specified.

It should be recalled that Equ.3 was derived on the assumption that $k(r_{max} - a) = n\pi$ for some integer n. Numerical evaluation for combinations of energy and r_{max} not obeying this relationship may be expected to differ from Equ.(3), i.e Equ.(3) will not be correct in such cases.

It should also be recalled that Equ.3 was derived using the zero-range approximation. We may expect, therefore, that numerical evaluations will agree better with Equ.3 if combinations of V_0 and a are employed in which a is small. Because of this we have used potentials with two different ranges, as follows,

Effective n-p Nuclear Potentials

	Singlet		**Triplet**		
	V_0 (MeV)	**a (fm)**	**V_0 (MeV)**	**a (fm)**	**B**
experimental	16.1	2.4	35.08	2.054	2.20759
reduced ‘a’	99.2	1.0	123.27	1.0	2.19328

The first line gives values (from Evans) derived from experimental data, and hence are best estimates. The second line gives equivalent potentials with the range reduced to 1 fm. For the triplet state, V_0 was first found from a = 1fm using the exact solution for a square well potential to reproduce the binding energy of 2.2245MeV. The last column of the Table gives the binding energies derived from the program NSW1a for the stated triplet potentials. They are close enough to the true value for our purposes. Note that there is no bound singlet state and $\tilde{B}$ is not a binding energy. Finally, the singlet potential for a = 1 fm was found using the energy quantisation expression for a square well, i.e. $a\tilde{\alpha}\cot(a\tilde{\alpha}) = -a\tilde{\beta}$, where $(\hbar\tilde{\alpha})^2 = 2m(V_0 - \tilde{B})$ and $(\hbar\tilde{\beta})^2 = 2m\tilde{B}$, whilst noting that this is not a bound state because $\tilde{\beta}$ is negative.

The following Table compares the numerical results of NSW1b with Equ.3 for the a = 1 fm potentials. Equ.3 is evaluated using the binding energy compatible with the program, i.e. B = 2.19328MeV. Results are presented for r_{max} = 57.32fm. We have not respected the requirement $k(r_{max} - a) = n\pi$, so this may introduce some of the differences observed. For the lowest energies calculated, the wavelength of the free state ($2\pi/k$) is far greater than r_{max}, and this would introduce serious error in the numerical results if special precautions were not taken. For the low energy cases (in italics in the Table) NSW1b applies a correction to the normalisation of the free state. Details are given in a note at the end of this Appendix. *This was never added.*

Matrix Elements $\langle {}^3S(\text{bound}) | {}^1S(\text{free}) \rangle$ **For n-p System**

(r_{max} = 57.32fm, No Coulomb Potential, Nuclear Potentials with a = 1fm)

E (MeV)	M.E. (from NSW1b)	M.E. (Equ.3)
0.0015625	*0.0921*	0.0937
0.003125	*0.1288*	0.1311
0.00625	*0.1783*	0.1815
0.0125	*0.2422*	0.2465
0.025	*0.3185*	0.3241
0.05	*0.3986*	0.4050
0.074		0.4462
0.125	0.4879	0.4892
0.25	*0.5181*	0.5146
0.5	0.5008	0.4960
1.0	0.4422	0.4326
2.0	0.3399	0.3352
4.0	0.2316	0.2292
8.0	0.1414	0.1398
16.0	0.0782	0.0785
32.0	0.0417	0.0418
64.0	0.0210	0.0216
128.0		0.0110

Note that at small energies the matrix element drops to zero proportional to $\sqrt{E}$. At large energies the matrix element also drops to zero, proportional to 1/E. Graphical plots of these results follow…

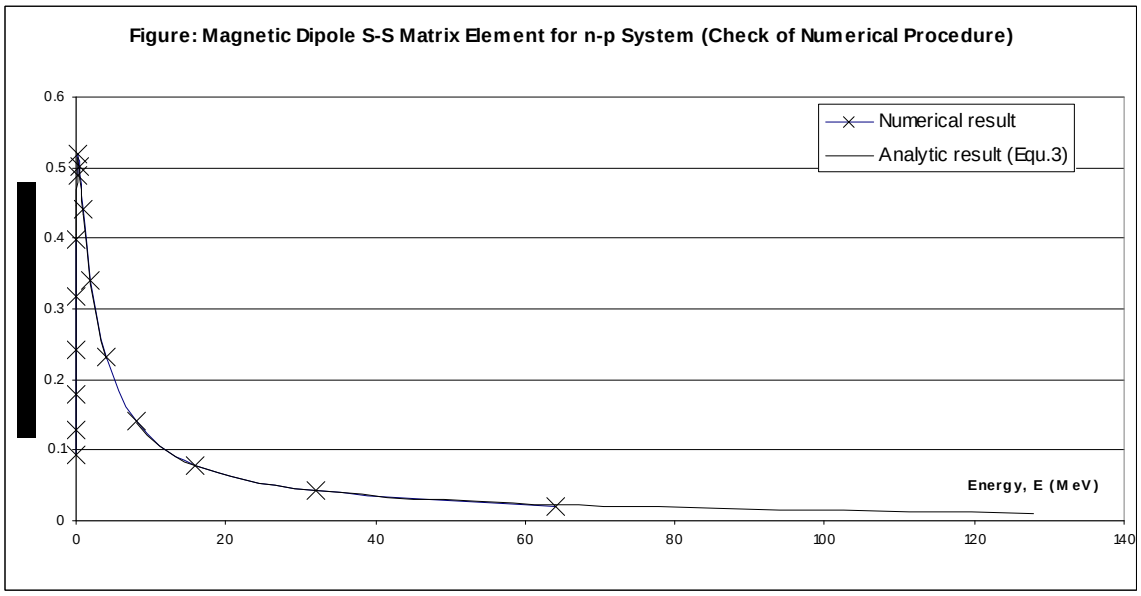

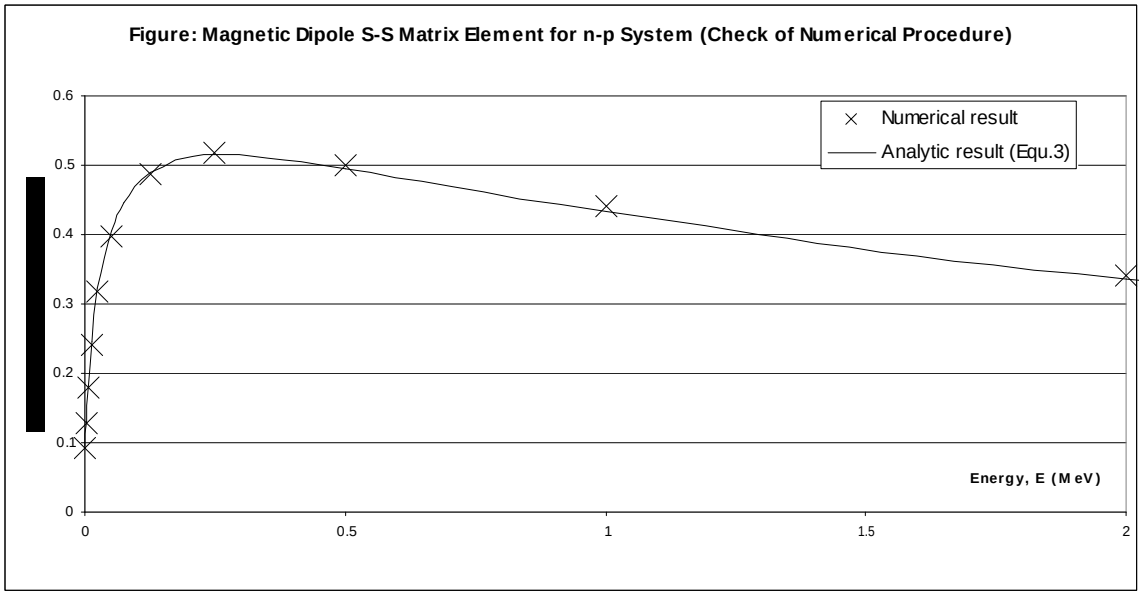

4.1.2 Check of $<^3 \mathrm{S(bound)}|r\cos\theta|^3 \mathrm{P(free)}>$ For The n-p Potentials

Appendix A2 has also derived an analytic expression for this electric dipole matrix element in the zero-range approximation, namely,

$$<^3 \mathrm{S(bound)}|r\cos\theta|^3 \mathrm{P(free)}>\Big|_{n-p} = \frac{4k^2}{\sqrt{3}\left(k^2+\beta^2\right)^2}\sqrt{\frac{\beta}{r_{max}}}\left(1+\frac{8}{\pi^2}\beta a\right)^{1/2} \quad \text{(Equ.4)}$$

Numerical and graphical results from the numerical integration program NSW1b are compared with Equ.4 as follows, for V0 = 123.27MeV and a = 1fm,

Matrix Elements $<^3 \mathrm{S(bound)}|r\cos\theta|^3 \mathrm{P(free)}>$ **For n-p System**

(r_{max} = 49.6fm, No Coulomb Potential, Nuclear Potentials with a = 1fm)

E (MeV)	M.E. (from NSW1b)	M.E. (Equ.4)
0.00625	*0.00946*	0.0092
0.0125	*0.01882*	0.0183
0.025	*0.03723*	0.0362
0.05		0.0707
0.1	*0.1395*	0.1353
0.2		0.2486
0.3	0.3549	0.3435
0.5	*0.5071*	0.4908
1	0.7257	0.6981
2	0.8399	0.8098
2.19328	0.8586	0.8115
2.5	0.8496	0.8081
3	0.8046	0.7920
5	0.7134	0.6880
10	0.5025	0.4789
20	0.3004	0.2891
40	0.1640	0.1600
100	0.06025	0.0682
200		0.0348

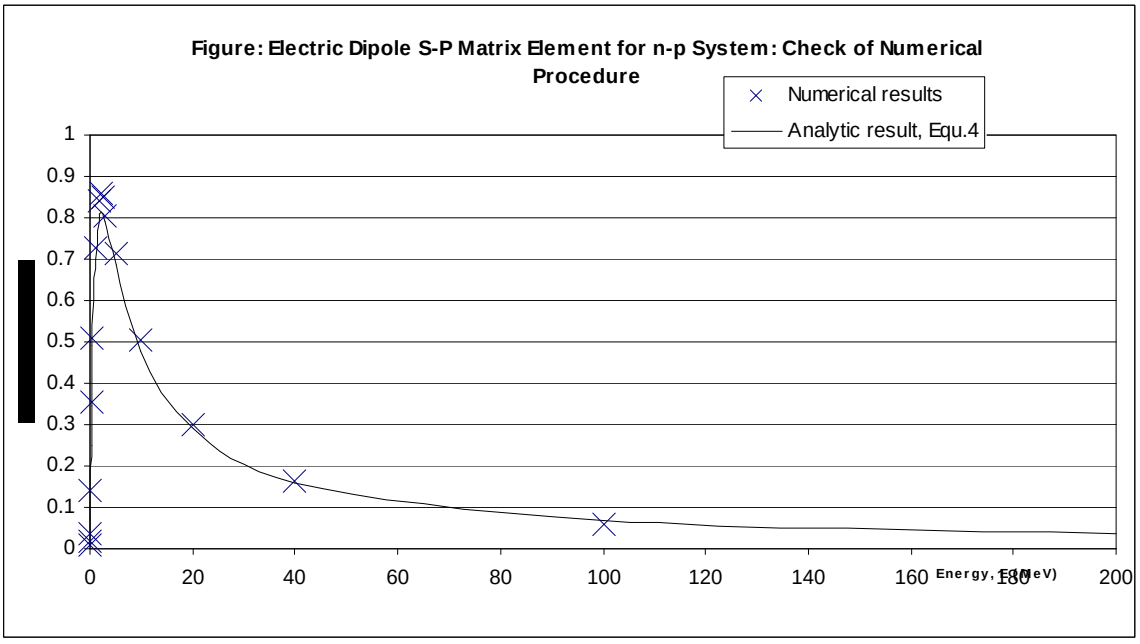

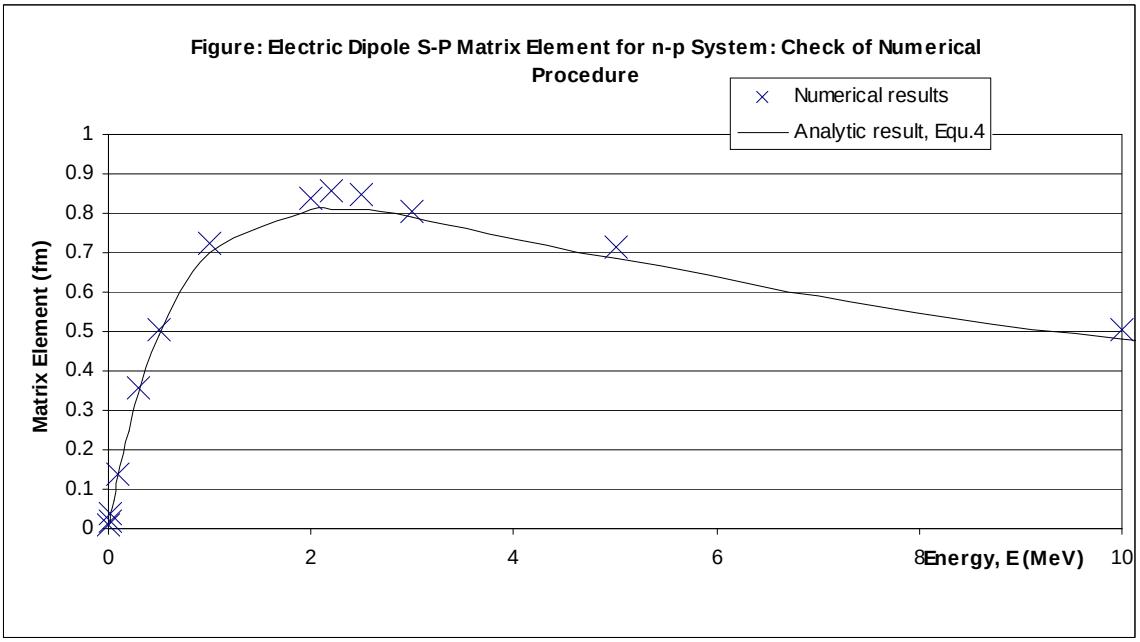

The matrix element again falls off as 1/E at large energy, but at small energies the drop-off is less steep than for the S-S matrix element, falling proportionally to E.

4.1.3 Sensitivity of n-p Matrix Elements to Coulomb Potential

To gain an impression for the sensitivity of a matrix element to switching on the Coulomb potential, we consider the n-p system as if a Coulomb potential applied. This may be thought of as being what the p-p matrix elements would be if the exclusion principle did not forbid their existence.

4.1.3.1 $<^3 S(\text{bound})|^1 S(\text{free})>$ With Coulomb Potential

For comparison, we use the same singlet and triplet potentials as in Section 4.1.1, namely $V_0 = 99.2$ MeV, $V_0 = 123.27$ MeV respectively, with a = 1 fm. The Coulomb potential is switched on only for r > a and is $V(r) = \tilde{e}^2 / r$, where $\tilde{e}^2 = 1.44\,\text{MeV.fm}$. The switching-on of the Coulomb potential changes the bound state binding energy from 2.19328 MeV to 1.68504 MeV. [I found it surprising, initially, that the Coulomb potential causes the binding energy to decrease rather than increase. This was because the Coulomb potential causes the apparent depth of the potential well to increase from V_0 to $V_0 + V_c$, where $V_c = \tilde{e}^2 / a$. However, it must be remembered that the bulk of the wavefunction lies outside the region of the nuclear potential, i.e. it is far more likely to find the nucleons spaced by r > a. The effective force of attraction is therefore the nuclear force *minus* the repulsive Coulomb potential. Clearly this will weaken the binding].

In the Table below we compare the numerical results from program NSW1b with the analytic result of Equ.(3). The latter does <u>not</u> account for the Coulomb potential. However, we use the shifted binding energy (B = 1.68504 MeV) in Equ.(3). This roughly accounts for the Coulomb effect on the bound state in Equ.(3), but there is no such allowance for the free state. In the numerical results from NSW1b we have used r_{max} = 57.32 fm. However, for small energies, NSW1b normalises the free states by using an extended radial integration, up to a radius which is given by,

$$r_{norm} = N_{norm}\left\{\frac{\tilde{e}^2}{E} + \frac{\pi\hbar}{\sqrt{2mE}}\right\} \qquad \text{(Equ.5)}$$

where N_{norm} is some positive integer, a value of 4 having been generally used here. Although NSW1b uses this increased integration range, the resulting normalisation constant is rescaled as if the normalisation had been to radius r_{max}, i.e. the wavefunction is multiplied by $\sqrt{r_{norm} / r_{max}}$. Hence, r_{max} may be deployed hereafter as if it had been the normalisation radius, and the matrix elements etc for small energies can be compared directly with those at higher energies.

E (MeV)	Equ.(3): Coulomb Barrier Not Present	NSW1b With Coulomb Barrier
5	0.1782	0.2159
2	0.3199	0.3892
1	0.4314	0.4978
0.5	0.5127	0.5025
0.25	0.5449	0.3839
0.125	0.5254	0.231
0.05	0.4391	0.0923
0.025	0.3525	0.0385
0.0125	0.2686	0.0126
0.00625	0.1979	0.00283
0.003125	0.1430	0.000369
0.0015	0.1002	1.87E-5
0.00075	0.0713	3.8E-7

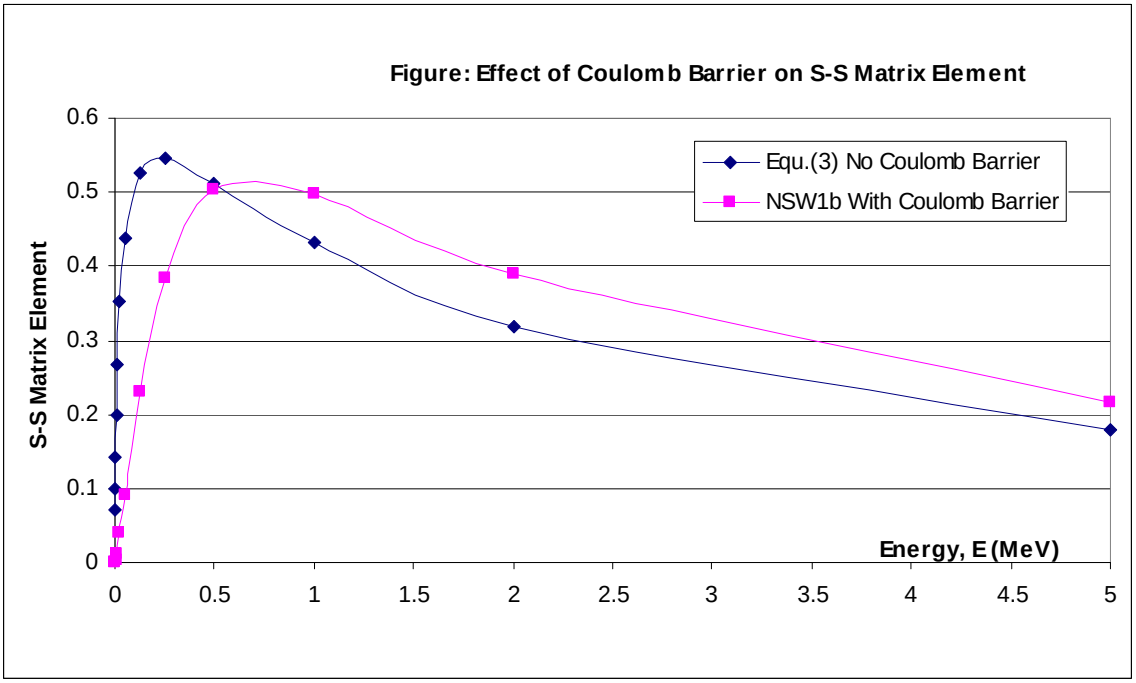

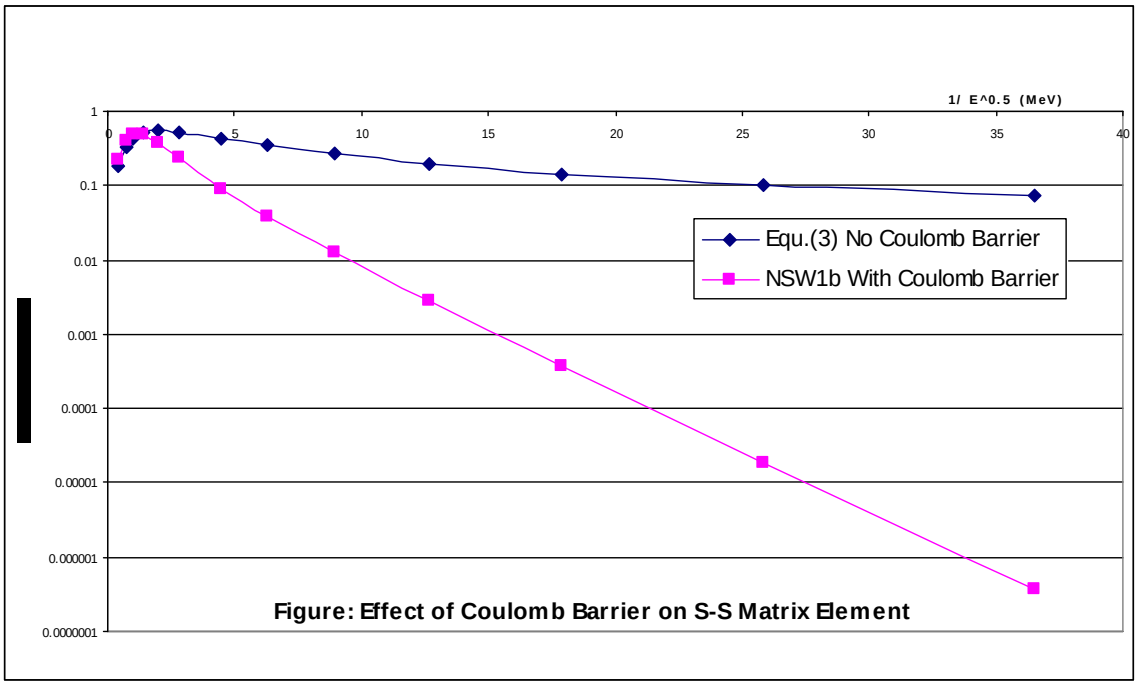

Figure: Effect of Coulomb Barrier on S-S Matrix Element

We have already seen that the matrix element without a Coulomb barrier reduces to zero at low energies proportionally to √E. The above logarithmic plot shows that at the lowest energies, the matrix element with the Coulomb barrier varies as $e^{-b/\sqrt{E}}$. The graph shows that b → 0.369 √MeV. This energy dependence can be derived simply as follows. Firstly, we note that the bound state wavefunction is little changed by the presence of the Coulomb potential:-

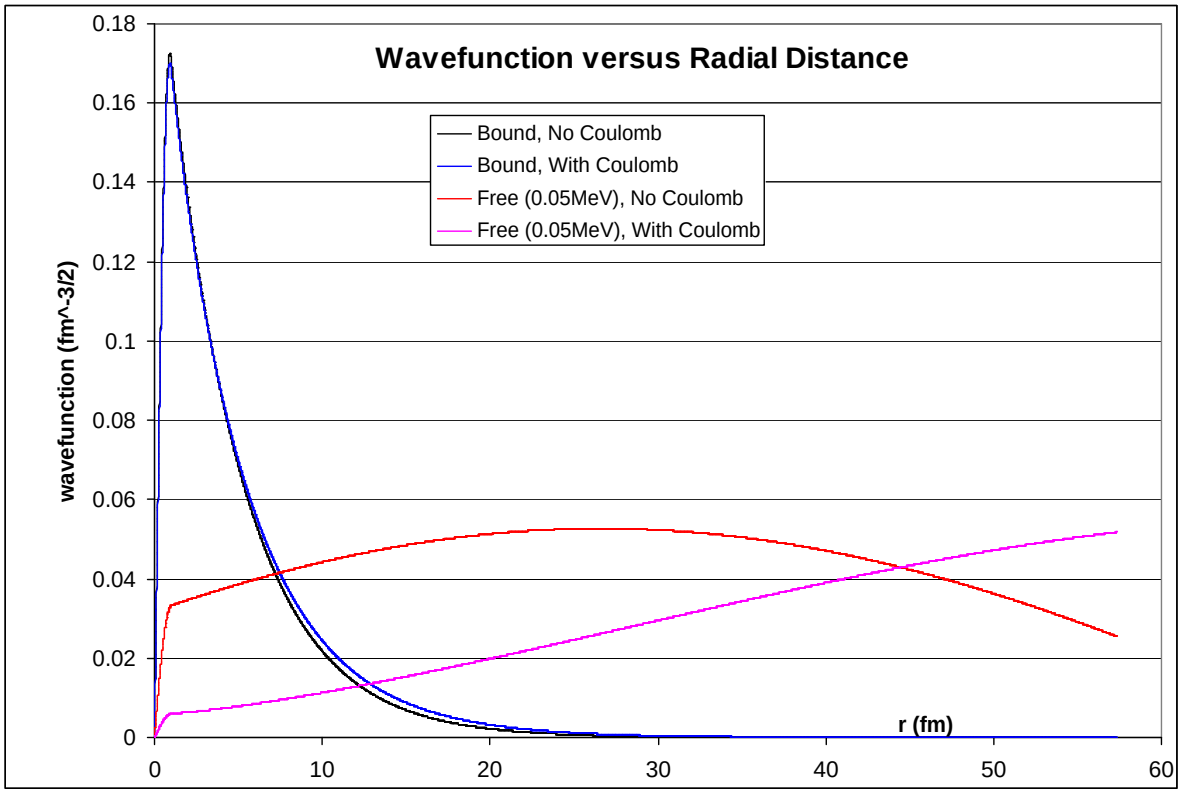

In contrast, the free state wavefunction is markedly reduced by the Coulomb potential. (The above illustration is for a free state energy of E = 0.05 MeV).

The reason for the marked change in the free state wavefunction is simply that, with the Coulomb potential switched on, the free state has negative kinetic energy (i.e. has exponential radial dependence rather than oscillatory) for r < 28.8 fm. This leads to the free state wavefunction being far smaller in the region where the bound state wavefunction is significant (i.e. r < 20 fm). In the above example with E = 0.05 MeV, it is smaller by a factor of ~4. It is simply this which results in the matrix element being smaller by a similar factor.

The above graph also illustrates clearly that most of the contribution to the matrix element comes from ***outside*** the range of the nuclear forces (i.e. from r > a = 1fm in this case).

Having made this observation, we now realise that energy dependence of the matrix element must derive from that of the free state in the region r < 20 fm, and hence depend essential on 'how much' of the free state manages to "penetrate the Coulomb barrier" from outside. Note, though, that this does not mean "how much of the free state exists in the interior region r < a". We have seen that very little does, at any energy, and indeed this is the basis of the zero-range approximation. It is actually the size of the free wavefunction within the region where the Coulomb potential is significant ($a < r < r_E = \tilde{e}^2 / E$) that matters. This is the region within which the free state has negative kinetic energy, the exponential decay length being (the reciprocal of) $\kappa = \sqrt{2m(V(r) - E)}/\hbar$, noting that this varies with 'r'. Roughly speaking, we may expect the magnitude of the wavefunction to diminish from r = r_E to r = a by a factor of $e^{-\int_a^{r_E} \kappa dr}$. The integral may be evaluated exactly to give a factor,

(Equ.6)

$$X = \exp\left\{ -\frac{\tilde{e}^2\sqrt{2m}}{\hbar} \cdot \frac{1}{\sqrt{E}} \left[\theta - \frac{1}{2}\sin 2\theta \right] \right\} \quad \text{where, } \theta = \tan^{-1}\sqrt{\frac{V_c}{E} - 1},\ V_c = \frac{\tilde{e}^2}{a}$$

For energies sufficiently small compared with V_c, $\theta \to \pi/2$ and hence the sin term is zero and we get,

$$X \to \exp\left\{ -b/\sqrt{E} \right\} \quad \text{where, } b = \frac{\pi\tilde{e}^2\sqrt{2m}}{2\hbar} = 0.351\sqrt{\text{MeV}} \text{ (for "p-p")} \qquad \text{(Equ.7)}$$

hence deriving the functional dependence on energy seen in the numerical results, and also confirming that the numerical value for b given above is very close to the expected value. This validates the numerical procedure of program NSW1b.

4.1.3.2 $<^3 S(\text{bound})|r\cos\theta|^3 P(\text{free})>$ **With Coulomb Potential**

Since the p-D cross section will require the S(spin ½)-P(spin ½) matrix element, we also examine the sensitivity of the n-p system matrix element to turning on the Coulomb potential. [The same remarks apply as in Section 4.1.3.1, namely that this

does not correspond to any actual physical process]. In this case we use the best estimate triplet potential (for both free and bound states), i.e. V_0 = 35.08 MeV and a = 2.054 fm and r_{max} = 57.32 fm. Program NSW1a gives the bound state binding energy when the Coulomb potential is switched on to be 1.94702 MeV. The comparison between the numerical results of program NSW1b, with the Coulomb potential on, and Equ.4 (which does not account for the Coulomb barrier – although we use the amended binding energy) is given by the following Table and graphs,

E (MeV)	**Equ.(3): Coulomb Barrier Not Present**	**NSW1b With Coulomb Barrier**
10	0.4824	0.5438
7.5	0.5786	0.6516
5	0.7133	0.7671
3	0.8440	0.8988
2.2	0.8808	0.8930
1	0.7928	0.7532
0.5	0.5749	0.5058
0.25	0.3566	0.2820
0.1	0.1643	0.1049
0.05	0.08632	0.04202
0.025	0.04426	0.01396
0.0125	0.02241	0.003865
0.00625	0.01128	0.000756
0.003125	0.005658	9.28E-5
0.0015	0.002720	4.46E-6
0.00075	0.001361	8.64E-8

Again it can be seen , from the second graph below, that the matrix element varies with energy, at sufficiently small energies, proportionally to $e^{-b/\sqrt{E}}$ and the numerical results give b ~ 0.369 from the last two data points, in good agreement with the theoretical estimate derived above.

Figure: Comparison of S-P Matrix Element With and Without Coulomb Barrier

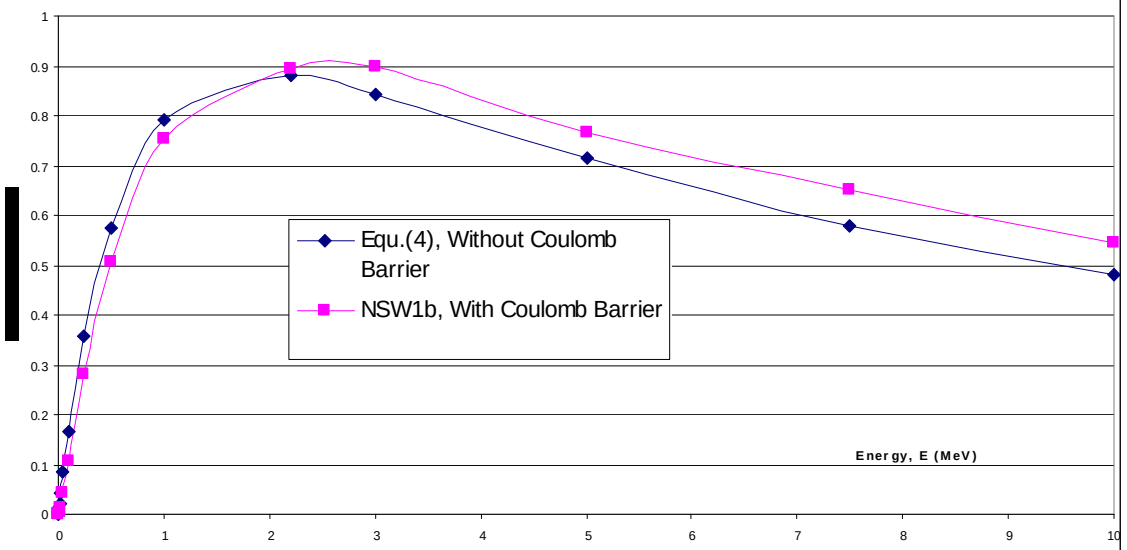

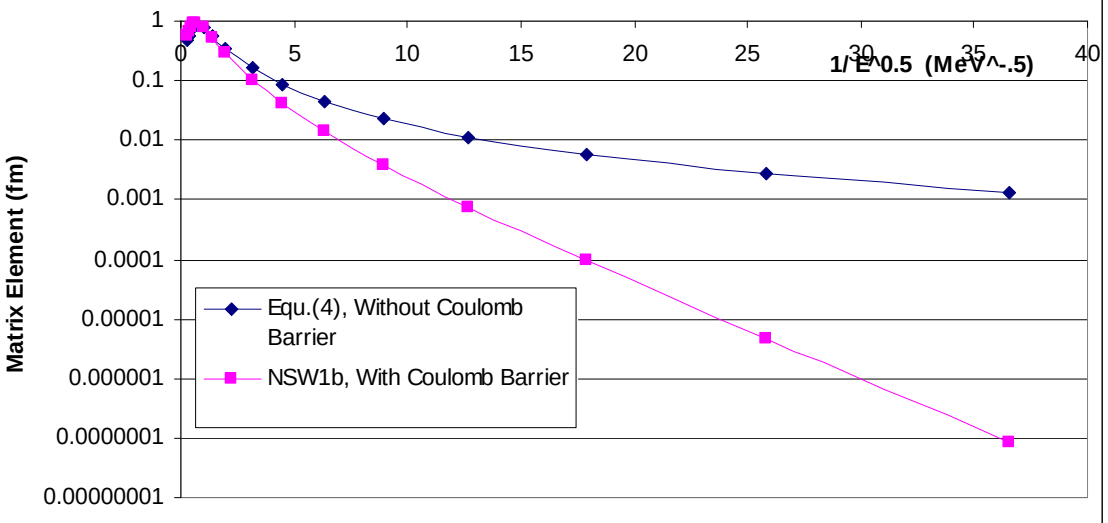

Figure: Comparison of S-P Matrix Element With and Without Coulomb Barrier

4.2 Derivation of the p-D Matrix Element

Having established the technique, NSW1b is now used together with the effective nuclear potentials of Section 3 to evaluate the matrix element for the p-D system. We choose (arbitrarily) the a = 2 fm potential with V_0 = 40.14 MeV. The Table below gives the matrix element (in fm) as a function of energy. Equ.4 is also shown for comparison, using the helium-3 binding energy (7.718 MeV). The reduced mass is m = 625.515 MeV, and the reference normalisation radius is r_{max} = 57.32 fm, as used above. (Note that the actual normalisation is carried out over a greater radius for low energy free states, see above discussion).

Values of $< \text{spin}^{1}/_{2}, \text{S(bound)} | r\cos\theta | \text{spin}^{1}/_{2}, \text{P(free)} >$ **for the p-D System (fm)**

E (MeV)	**matrix element (fm) from NSW1b (with Coulomb barrier)**	**matrix element (fm) from Equ.4 (no Coulomb barrier)**
100	0.003202	0.07776
60	0.02668	0.1181
40	0.07380	0.1585
20	0.2619	0.2349
10	0.4301	0.2874
7.71779 (B)	0.4361	0.2923
5	0.3959	0.2789
2	0.2455	0.1911
1	0.1362	0.1187
0.72 (V_c)	0.09995	0.09124
0.5	0.06915	0.06880
0.25	0.03229	0.03553
0.1	0.01036	0.01476
0.05	0.003757	0.007477
0.02	0.00075	0.00301
0.01	0.000164	0.001511
0.005	2.32E-5	0.000756
0.002	5.99E-7	0.000303
0.001	1.16E-8	0.0001511
0.0005	4.73E-11	0.000076

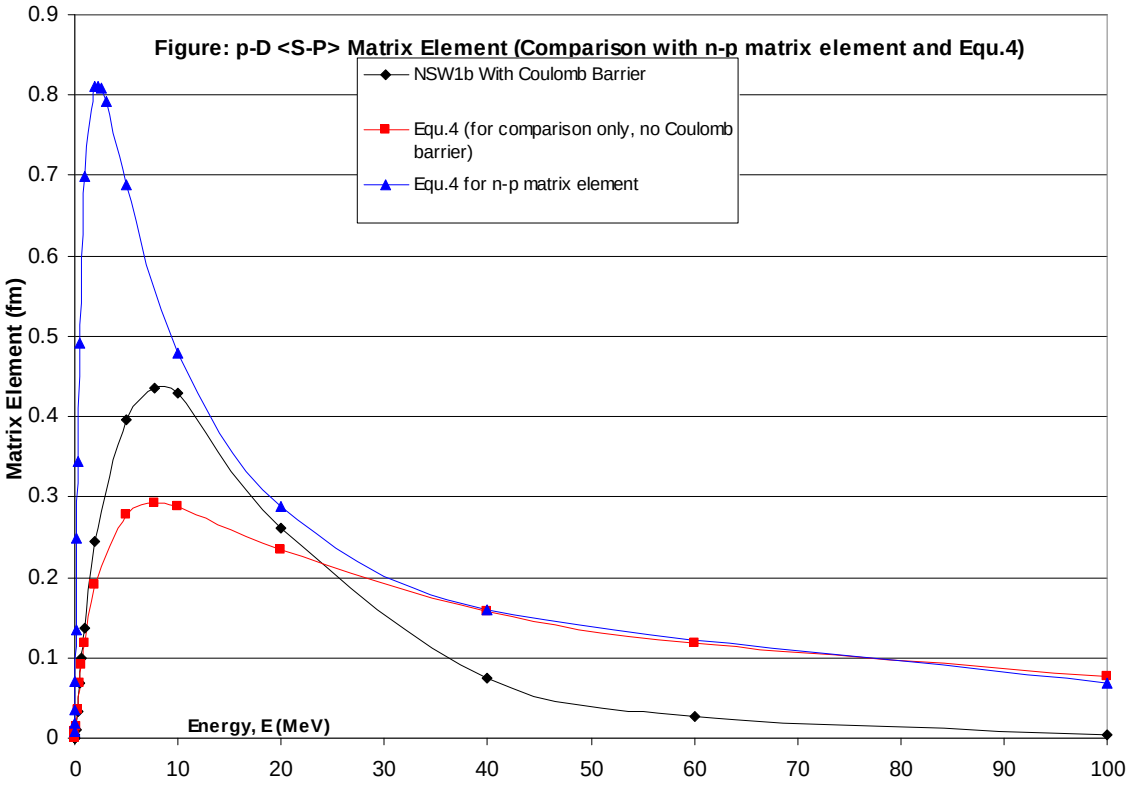

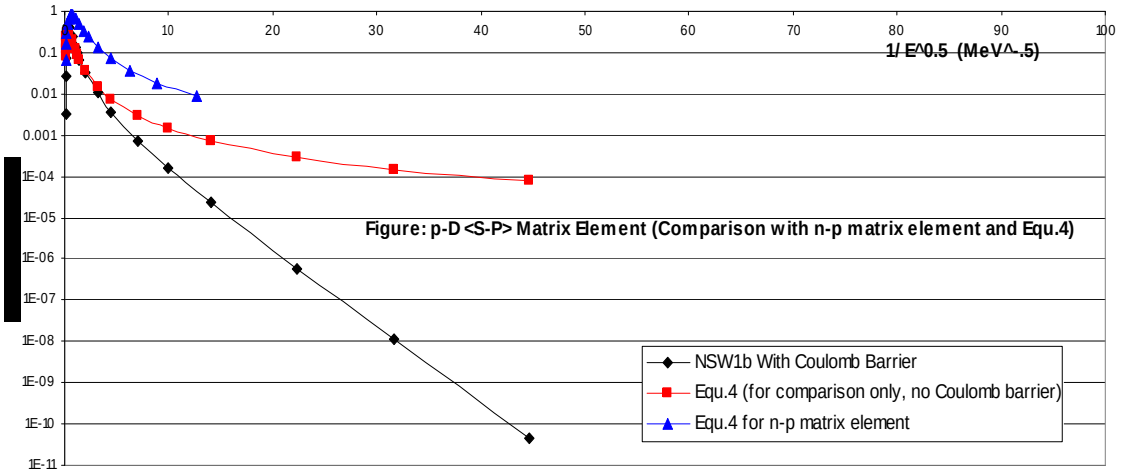

The graphs show that there is a band of energies (roughly 12 to 25 MeV) where the n-p and p-D matrix elements are of similar magnitude, but that for other energies the p-D matrix element tends to be much smaller. Its largest value is about half that for n-p. At sufficiently large and sufficiently small energies, the p-D matrix element is orders of magnitude smaller than that for n-p. At low energies, this is the result of the Coulomb barrier. The last pair of data points gives a value b = 0.420 for the parameter in the energy factor $e^{-b/\sqrt{E}}$. This compares with the theoretical estimate of 0.405 from Equ.7 (recalling that p-D has a larger reduced mass than n-p). Hence, the low energy behaviour conforms to expectation.

The reason for the steeper reduction in the matrix element at high energies is unclear.

5. Calculation of the p + D → ^{3}He + γ Reaction Rate at a Given Temperature

Following Appendix A2, the reaction rate for the photodisintegration reaction ^{3}He + γ → p + D is,

$$w = 2 \cdot \left(\frac{2\pi}{\hbar}\right)\left(\frac{mr_{max}}{\pi\hbar^2 k}\right)(eE_0)^2 \left| < S(bound) \left| r\cos\theta \right| P(free) > \right|^2 \qquad \text{(Equ.8)}$$

and w is the probability of disintegration per second per helium-3 nucleus. The second term in brackets in Equ.8 is the density of final states. For the numerical values of the matrix element given above we must use, for consistency, r_{max} = 57.32 fm.

The leading factor of two accounts for the fact that the photon may couple to either of the two protons, and hence doubles the reaction rate. [There is a problem of principle here. If the helium-3 is regarded as a particle of charge 2e, then the matrix element involves $(2eE_0)^2$, and this results in double the reaction rate given by Equ.8. Why is it not correct to do the calculation this way? We note that at the photon energies involved, i.e. ~5.5MeV or above, the photon wavelength is ~220fm, and so the photon cannot resolve the two protons. It may be that Equ.8 is wrong and should be multiplied by 2].

Recall from Appendix A2 that the cross-section, photon flux and fine structure constant are given by,

$$\sigma_{dis} = \frac{w}{J_\gamma^N} \quad \text{and} \quad J_\gamma^N = \frac{2E_0^2}{\hbar\omega c\mu_0} \quad \text{and} \quad \alpha = \frac{c\mu_0 e^2}{4\pi\hbar} \qquad \text{(Equ.9)}$$

where $\hbar\omega$ is the photon energy. Hence, Equ.8 gives,

$$\sigma_{dis} = 8\pi\alpha \frac{m\omega r_{max}}{\hbar k} \left| < S(bound) \left| r\cos\theta \right| P(free) > \right|^2 \qquad \text{(Equ.10)}$$

We noted in Appendix A2 that our derivation of the electric dipole cross-section was too large by a mysterious factor of 4 which we failed to trace. Anticipating that the same error occurs here, we re-write Equ.10 as,

$$\sigma_{dis} = 2\pi\alpha \frac{m\omega r_{max}}{\hbar k} \left| < S(bound) \left| r\cos\theta \right| P(free) > \right|^2 \qquad \text{(Equ.10)}$$

Inserting the values of the constants into Equ.10 gives,

$$\sigma_{dis} = 8.32\left(\frac{\omega}{kc}\right) \left| < S(bound) \left| r\cos\theta \right| P(free) > \right|^2 \qquad \text{(Equ.11)}$$

It is the matrix element in Equ.11 which carries the dimensions. Thus if the matrix element is evaluated in fm (as in the above numerical data) the cross-section is in fm^2 = 0.01 barn. To calculate the capture cross-section we use,

$$\frac{\sigma\left(p + D \rightarrow {}^3\,He + \gamma\right)}{\sigma\left({}^3He + \gamma \rightarrow p + D\right)} = \frac{\text{number of } {}^3He + \gamma \text{ spin states}}{\text{number of } p + D \text{ spin states}} \left[\frac{p_\gamma}{p_p}\right]^2 = \frac{2}{3}\left[\frac{p_\gamma}{p_p}\right]^2 \qquad \text{(Equ.12)}$$

In the centre of mass system, the proton and deuteron momenta are equal and opposite and both equal in magnitude to $\hbar k = \sqrt{2mE}$, where m is the reduced mass and E is the sum of the proton and deuteron kinetic energies in the CoM system. For the low photon energies in question, i.e. not much more than the minimum to cause photodisintegration, the kinetic energy of the helium-3 nucleus is negligible (about 0.1% of that of the photon). Thus, the energy of the photon released by proton capture is given accurately by E plus the difference of the binding energies of helium-3 and the deuteron, i.e. $\Delta B = 7.718 - 2.2225 = 5.4956 MeV$. Hence the factors which occur in Equs.11 and 12 are,

$$\frac{p_\gamma}{p_p} = \frac{\omega}{kc} = \frac{E + \Delta B}{\sqrt{2mc^2 E}} \qquad \text{(Equ.13)}$$

So Equs.11, 12, 13 give,

$$\sigma_{cap} = 5.55\left(\frac{E + \Delta B}{\sqrt{2mc^2 E}}\right)^3 \left| < S(\text{bound}) \right| r\cos\theta \left| P(\text{free}) > \right|^2 \qquad \text{(Equ.14)}$$

Thus, if we consider there to be a density of deuterons of 1 mole per cm^3 (i.e. $\rho_D^N = 6.02x10^{29}\, m^{-3}$), then the number of capture reactions per m^3 per second per proton is,

$$\text{Reaction Rate} = 6.02x10^{29}\, v\sigma_{cap} \qquad \text{(Equ.15)}$$

where v is the relative closing speed of the proton and deuteron. Thus Equ.15, together with Equ.14, suffice to find the reaction rate if we know the relative speed (v) of the reactants in the laboratory frame of reference, and we know the total kinetic energy (E) in the CoM frame. Unfortunately, for a gas of protons and deuterons in thermal equilibrium there is a continuous distribution of these variables. For the non-relativistic energies of interest, the energies are given by the Maxwell distribution,

$$P[\varepsilon]d\varepsilon = \frac{2}{\sqrt{\pi}}\sqrt{\varepsilon}e^{-\varepsilon}d\varepsilon \qquad \text{(Equ.16)}$$

where $\varepsilon = E/kT$ and the distribution applies to both the proton and the deuteron. We denote the reaction rate at temperature T by R[T]. Conversely, if all the protons had speed v_p in the lab frame, and all the deuterons speed v_D, and the two velocities were at an angle θ, the resulting reaction rate is denoted $R[v_p, v_D, \theta]$. If we know the latter we can find R[T] from,

$$R[T] = \int_0^\infty P[\varepsilon_p]d\varepsilon_p \int_0^\infty P[\varepsilon_D]d\varepsilon_D \int_0^\pi \frac{d(\cos\theta)}{2} \cdot R[v_p, v_D, \theta] \qquad \text{(Equ.17)}$$

where, $\varepsilon_p = \frac{M_p v_p^2}{2kT}$ and $\varepsilon_D = \frac{M_D v_D^2}{2kT} = \frac{M_p v_D^2}{kT}$. Because the random motions are isotropic, all solid angles are equally likely, hence the uniform probability density in $\cos\theta$. Now $R[v_p, v_D, \theta]$ will be given by Equs.14, 15 provided we can find the lab frame relative speed (v) and the CoM system total energy (E) in terms of v_p, v_D and θ. In the (very good) approximation that the deuteron is twice the mass of the proton, it is simple to show that,

$$v^2 = v_p^2 + v_D^2 - 2v_p v_D \cos\theta \quad \text{and} \qquad E = \frac{1}{3}M_p v^2 \qquad \text{(Equ.18)}$$

Thus, the reaction rate at temperature T can be found by numerically integrating Equ.17 using Equs.14, 15, 16 and 18. The results are compared with the reaction rates given by Hoffman et al in the Table below,

Temperature (K)	**Reaction Rate, Equ.17** s^{-1} per mole/cm^3	**Reaction Rate, Hoffman et al** s^{-1} per mole/cm^3
10^7	0.001	-
1.4×10^7	0.0053	*0.0036*[(1)]
3×10^7	0.127	0.21
5×10^7	0.71	1.10
10^8	5.0	7.0
3×10^8	59	65
5×10^8	151	150
10^9	461	390
1.5×10^9	831	630
2×10^9	1239	870

[(1)] *Unreliable extrapolation*

Although the agreement at individual temperatures is not always impressive, this is partly because the reaction rate is so sensitive to temperature. Overall the agreement is remarkably good given the simplicity of our treatment, as the following graph shows,

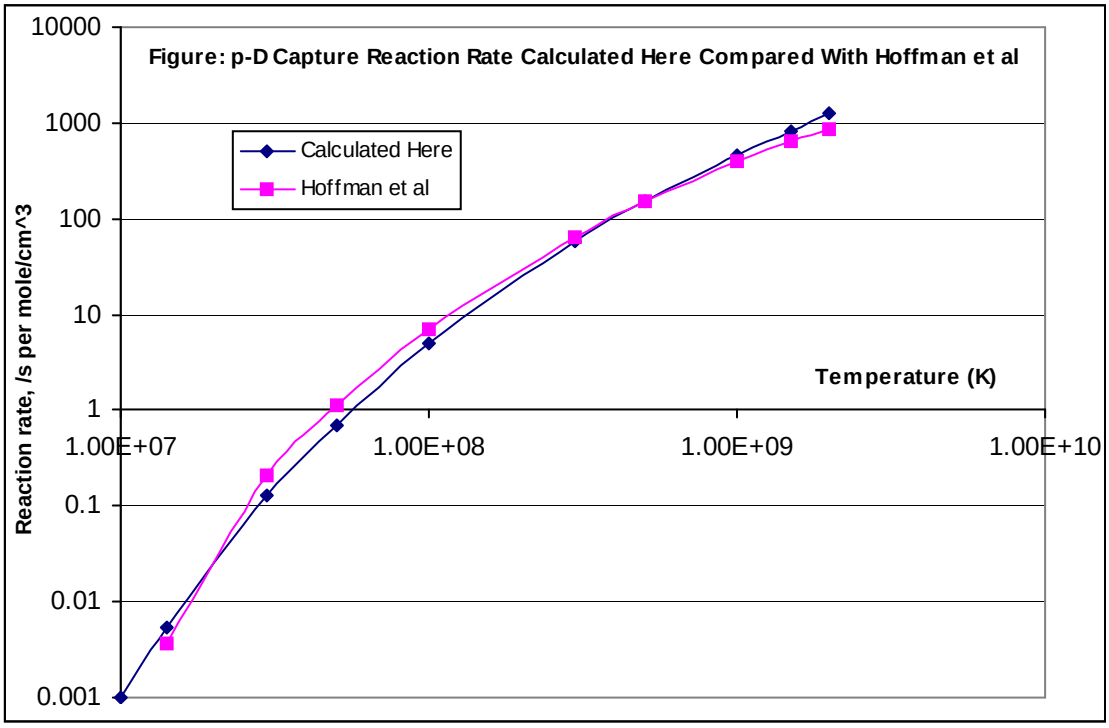

6. Discussion of the Temperature Dependence of the Reaction Rate

If we examine the temperature dependence of the predicted reaction rates given in the above table/graph (using Equ.17 rather than Hoffman, for definiteness) we see that fitting to the functional form Rate $\propto \exp\{-b/\sqrt{< E >}\}$, where the mean energy is 1.5kT, we get numerical values for b of about 0.385 at ~10^7 K, rising to ~0.82 at ~4 x 10^8 K. It is important to realise that the reaction rate at a given temperature does not derive only from the energy dependence of the matrix element. The latter has a 'b' parameter of ~0.405, and because it is squared in the expression for cross-section, would imply a reaction rate energy dependence with b ~ 0.81 if there were no other sources of energy dependence.

In fact there are three other sources of temperature dependence. The first two are displayed in Equs.(14) and (15). Thus, if we consider low energies, E << B, then Equ.(14) has a factor of $E^{3/2}$ in the denominator, in addition to the energy dependent matrix element. Euq.(15) introduces further energy dependence via the velocity factor. Ignoring the complication of θ dependence, the velocity varies essentially as √E. Hence, combining Equs(14) and (15) we have a net factor of 1/E.

However, the third source of temperature dependence is the most important, namely the Maxwell distribution of energies at a given temperature. This is displayed explicitly in Equs.(16, 17, 18). In the numerical evaluation, above, we have correctly accounted for all three of these temperature dependencies. They are the reason why the fitted 'b' parameter is not simply twice that for the matrix element. It is instructive to attempt an approximate analytic derivation of the temperature dependence of the reaction rate. From the above discussion, ignoring the complication of the θ dependence, and assuming the energy dependence of the matrix element can be

approximated as $\propto \exp\{-b/2\sqrt{E}\}$, we expect the temperature dependence of the reaction rate at temperature T to be proportional to,

$$\text{Reaction rate} \propto \int_0^\infty\int_0^\infty \frac{dE_1 dE_2}{(kT)^3}\frac{\sqrt{E_1E_2}}{E_1+E_2}\exp-\left\{\frac{b}{\sqrt{E_1+E_2}}+\frac{E_1+E_2}{kT}\right\}$$

$$\propto \int_0^\infty \frac{dy}{(kT)^3}\frac{\exp-\left\{\frac{b}{\sqrt{y}}+\frac{y}{kT}\right\}}{y}\int_{-y}^{+y}\sqrt{y^2-x^2}\,dx \qquad \text{(Equ.19)}$$

where, $y = E_1 + E_2 = E$, and $x = E_1 – E_2$. Note that the range of integration $E_1 \in [0, \infty]$ and $E_2 \in [0, \infty]$ maps into $y \in [0, \infty]$ and $x \in [-y, +y]$, since $E_1 = (x + y)/2$ and $E_2 = (y – x)/2$. Also note that the parameter ‘b’ in the above is twice that applying for the matrix element, and hence is ~0.81 for sufficiently small E. The second integral is just $\pi y^2/2$, so (19) becomes,

$$\text{Reaction rate} \propto \int_0^\infty \frac{dy}{(kT)^3}\,y\exp-\left\{\frac{b}{\sqrt{y}}+\frac{y}{kT}\right\} \qquad \text{(Equ.20)}$$

We can estimate (20) by expanding the exponent as a power series, noting that it attains a minimum when,

$$y_0 = E_0 = (0.5bkT)^{2/3} \qquad \text{(Equ.21)}$$

this being the energy which contributes most to the overall reaction rate. [NB: At lower energies the matrix element and hence the reaction rate reduces rapidly, whereas at higher energies the Maxwell distribution ensures that there are a rapidly reducing number of particles with such energies]. Thus,

$$f(y) = \frac{b}{\sqrt{y}}+\frac{y}{kT} \approx f_{min} + 0.5f_0''(y-y_0)^2 + ... \qquad \text{(Equ.22a)}$$

where, $f_{min} = \frac{3}{2^{2/3}}\cdot\frac{b^{2/3}}{(kT)^{1/3}}$ and $f_0'' = \frac{3}{4}by_0^{-5/2}$ (Equ.22b)

Thus, (20) is approximated as,

$$\text{Reaction rate} \propto \frac{y_0}{(kT)^3}e^{-f_{min}}\int_0^\infty \exp-\{0.5f_0''(y-y_0)^2\}dy \qquad \text{(Equ.23)}$$

$$\propto \frac{y_0}{(kT)^3} e^{-f_{min}} \cdot \lambda \cdot \sqrt{\frac{2\pi}{f_0''}}$$

$$\propto \frac{y_0}{(kT)^3} e^{-f_{min}} \sqrt{y_0^{5/2}}$$

$$\propto \frac{y_0^{9/4}}{(kT)^3} e^{-f_{min}} \qquad \text{(Equ.24)}$$

$$\propto \frac{\left[(kT)^{2/3}\right]^{9/4}}{(kT)^3} e^{-f_{min}}$$

$$\propto \frac{e^{-f_{min}}}{(kT)^{3/2}}$$

The dominant dependence is the exponential, but from Equ.(22b) we see that this is not a $\exp -\beta/\sqrt{E}$ factor but has a different energy dependence in the exponent, namely $f_{min} = \frac{3}{2^{2/3}} \cdot \frac{b^{2/3}}{(kT)^{1/3}}$. If we equate Equ.(24) to an effective term of the form $\exp -\beta/\sqrt{E}$, assuming b = 0.81, then the energy dependent parameter β varies as follows,

T (10^6 K)	**E = 1.5kT (MeV)**	**f_{min}** dimensionless	$\frac{e^{-f_{min}}}{(kT)^{3/2}}$ *	β **√MeV**
10	0.00129	17.27	0.0257	0.310
14	0.00181	15.43	0.0975	0.312
20	0.00259	13.69	0.325	0.313
25	0.00323	12.72	0.6157	0.315
30	0.00388	11.96	1.0	-

*Normalised by its value at T = 30 million K.

Thus, the effective 'b' parameter is ~0.31 for low temperatures, which compares with the numerical derivation above which implies that 'b' is around 0.385 – 0.426 for temperatures of 10 to 30 million K. The agreement is reasonable if not especially impressive. The main point, however, is that the above considerations explain why the effective 'b' differs markedly from twice the matrix element value for 'b', i.e. ~0.81. At higher temperatures the numerical derivation shows that 'b' increases, but our estimate, above, would not then be expected to be accurate since the matrix element then ceases to vary in the assumed manner.